DALTON

Copper(II) complexes with cyclo(L-aspartyl-L-aspartyl) and cyclo(L-glutamyl-L-glutamyl) derivatives and their antioxidant properties

Raffaele P. Bonomo,[a] Enrico Conte,[a] Giuseppe Impellizzeri,[a] Giuseppe Pappalardo,[b] Roberto Purrello[a] and Enrico Rizzarelli[a,b]

[a] *Dipartimento di Scienze Chimiche, V.le A. Doria 6, 95125, Catania, Italy*
[b] *Istituto per lo Studio delle Sostanze Naturali di Interesse Alimentare e Chimico-Farmaceutico, CNR, Via Del Santuario 110, 95028, Valverde (Catania), Italy*

Two new functionalized cyclodipeptides have been synthesized with the aim of obtaining a good model of superoxide dismutase. Better to mimic the active site of this metalloenzyme, these two compounds have been designed to allow a great co-ordination flexibility. Copper(II) complexes with cyclo(-L-aspartyl-L-aspartyl-) or cyclo(-L-glutamyl-L-glutamyl-)bis(histamine) (L) have been thermodynamically and spectroscopically characterized and their antioxidant activity tested against enzymatically generated O_2^-. Taking into account the speciation of the system, it has been determined that the more active species against O_2^- is the $[CuL_2]^{2+}$ complex. Electron spin resonance measurements suggest for this species the presence of four imidazole nitrogen atoms in a slightly tetrahedrally distorted co-ordination plane. The $[CuLH_{-2}]$ complex species also possesses four-nitrogen co-ordination involving two deprotonated peptide nitrogen atoms. The complex $[CuL_2]^{2+}$ showed the highest antioxidant activity and reasons for this behaviour are proposed on the basis of spectroscopic and voltammetric data.

The superoxide (hyperoxide) radical O_2^- is formed during the biological reduction of oxygen to water.[1-3] This very toxic species is thought to be involved in diseases and pathological processes, such as ageing,[4] cancer,[5] membrane damage,[6] DNA damage,[7] *etc.*[8] Cells are protected against this species by superoxide dismutase (SOD), a metalloenzyme which very efficiently catalyses the dismutation of superoxide radicals into hydrogen peroxide and molecular oxygen.[2] There are three known kinds of this enzyme: a copper–zinc protein found in eukaryote cells and manganese– or iron–zinc proteins mainly found in bacteria. The presence in the active site of a metal ion able to participate in a redox cycle is crucial for SOD catalysis, according to reactions (1) and (2) in which the metal ion is

$$Cu^{II} + O_2^- \rightleftharpoons Cu^{I} + O_2 \quad (1)$$

$$Cu^{I} + O_2^- + 2H^+ \rightleftharpoons Cu^{II} + H_2O_2 \quad (2)$$

reversibly reduced [equation (1)] and oxidized [equation (2)] by superoxide radicals.[9] The resolved structure of bovine SOD shows copper(II) co-ordinated to four histidines with an uneven tetrahedral distortion from a square-planar geometry.[10] Recently, an EXAFS (extended X-ray absorption fine structure) study has been carried out on the nickel-substituted Cu,Zn superoxide dismutase evidencing five-co-ordination for the nickel ion which took the place of zinc.[11] The distorted four-co-ordination geometry, unusual for copper(II) complexes but matching the geometrical demands of copper(I), has been proposed to be one of the factors which increases the redox potential of 'catalytic' copper(II) to a value much higher than that of aquacopper(II).[12] On the other hand, histidines are both good donors and acceptors and can stabilize both oxidation states achieved by copper in the SOD catalytic cycle. Therefore, both the histidine donor–acceptor nature and the flexibility of the co-ordination catalytic centre are necessary to obtain good metalloenzyme models. In order to achieve these goals we have designed and synthesized two new histamine(imidazole-4-ethanamine)-functionalized cyclodipeptides; namely cyclo(-L-aspartyl-L-aspartyl-) bis(histamine) L^1 and cyclo(-L-glutamyl-L-glutamyl-) bis(histamine) L^2. The advantage of having the diketopiperazine ring in these models is two-fold: (*i*) free carboxylate and amino terminal groups are not present as found in natural binding sites, (*ii*) the diketopiperazine 'rigid' structure is able to promote non-covalent interactions between the two functionalized arms, *i.e.* to promote 'preorganization'. Proton and copper(II) complexes of these species were studied by pH-metric measurements and ESR and UV/VIS spectroscopic data provided information about the peculiar geometries of the most relevant copper(II) species. Moreover, voltammetric measurements were carried out to investigate the SOD-like activity revealed by the enzymatic xanthine–xanthine oxidase test.

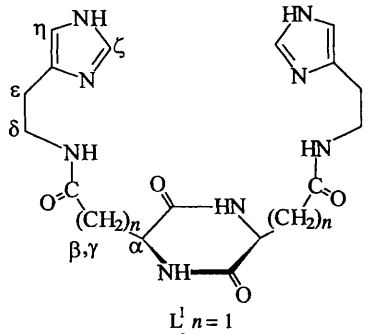

Experimental

Synthesis and materials

L^1. 1-Hydroxybenzotriazole (1 mmol) and benzotriazolyl-*N*-oxy-tris(dimethylamino)phosphonium hexafluorophosphate (1 mmol) were added to a solution of histamine (Aldrich) (1 mmol) and cyclo-(-Asp-Asp-) (Bachem) (0.43 mmol) dissolved in anhydrous dimethylformamide (dmf, 10 cm^3). The reaction mixture was stirred at room temperature overnight under a

nitrogen stream and then evaporated to dryness *in vacuo*. The white residue was dissolved in water and purified on a CM-Sephadex C-25 (NH_4^+ form) column by eluting initially with water and then with a gradient from 0 to 0.2 mol dm^{-3} aqueous ammonium hydrogencarbonate. The product was detected by TLC (thin-layer chromatography) with Pauli Spray reagent.[13] The appropriate fractions were combined and evaporated to dryness at 40 °C *in vacuo* to let ammonium hydrogencarbonate decompose. The desired product was obtained in good yield (0.38 mmol, yield 88%) and its purity was checked by TLC, $R_f = 0.18$ (SiO_2 plates, eluent PrOH-ethyl acetate–water–NH_3, 5.0:5.0:3.0:0.2 v/v); m.p. 235 °C (decomp.), $[\alpha]_D^{25}$ (° cm^2 g^{-1}) = −38 (*c* 0.5, water) FAB–mass spectrum: *m/z* 417 (MH^+) (Found: C, 52.00; H, 5.80; N, 26.80. Calc. for $C_{18}H_{24}N_8O_4$: C, 51.90; H, 5.80; N, 26.90%); The product identity was further confirmed by means of ^1H NMR and correlation spectroscopy (COSY) in D_2O at 250 MHz on a Bruker AC-250 spectrometer: δ 4.35 (t, 2 H, α-CH), 2.72 (m, 8 H, β-, ε-CH_2), 3.40 (m, 4 H, δ-CH_2), 6.87 (s, 2 H, η-CH) and 7.62 (s, 2 H, ζ-CH).

L^2. This compound was prepared by following the above procedure and utilizing cyclo(-Glu-Glu-) (Bachem) and histamine (Aldrich) (yield 90%). TLC: $R_f = 0.20$ (SiO_2 plates, eluent PrOH-ethyl acetate–water–NH_3 5.0:5.0:3.0:0.2 v/v). m.p. 261 °C (decomp.). $[\alpha]_D^{25} = -19°$ (*c*, 0.5, water). FAB mass spectrum: *m/z* 445 (MH^+) (Found: C, 54.60; H, 6.40; N, 25.10. Calc. for $C_{20}H_{28}N_8O_4$: C, 54.05; H, 6.35; N, 25.20%). ^1H NMR (D_2O) (the presence of an additional CH_2 group leads to further signals associated with the γ position): δ 4.03 (t, 2 H, α-CH), 2.02 (m, 4 H, β-CH_2), 2.25 (m, 4 H, γ-CH_2), 3.38 (t, 4 H, δ-CH_2), 2.72 (t, 4 H, ε-CH_2), 6.84 (s, 2 H, η-CH) and 7.61 (s, 2 H, ζ-CH).

Copper(II) nitrate was a 'reinst' Merck product. The concentration of the stock solution was determined by ethylenedinitrilotetraacetate titrations, using murexide as indicator.[14] Stock solutions of HNO_3 and KOH were made up from concentrated HNO_3 (Suprapur Merck) and from Normex (C. Erba) vials, respectively. Their concentrations were determined potentiometrically by titrating with tris-(hydroxymethyl)methylamine and potassium hydrogenphthalate, respectively. All solutions were prepared with freshly distilled (four times) CO_2-free water. The ionic strength was adjusted to 0.10 mol dm^{-3} by adding KNO_3 (Suprapur Merck). Grade A glassware was employed throughout. Xanthine, xanthine oxidase and nitro blue tetrazolium were from Sigma.

Electromotive force measurements

The potentiometric measurements were carried out by means of four fully automated sets of apparatus. These made use of Metrohm equipment (burette, E665; meter, E654; glass electrodes, EA 109; calomel electrodes, EA 404) and were controlled by an IBM-compatible personal computer. Each computer was able to control two potentiometric set-ups simultaneously by using a program written in our laboratory. All experiments were carried out at 25.0 ± 0.2 °C using thermostatted cells (5 cm^3). All solutions were magnetically stirred and maintained under an atmosphere of nitrogen previously bubbled through 0.1 mol dm^{-3} KNO_3 solutions. The electrode couples were standardized on the pH = $-\log c_{H^+}$ scale by titrating HNO_3 with CO_2-free KOH. The cyclopeptide concentration was kept in the range 4–8 mmol dm^{-3} and the copper(II) to cyclopeptide ratio was in the range 1–2:1 Totals of 283 and 342 experimental points were collected for copper(II)-L^1 and -L^2, respectively. Each experiment was simultaneously run in both potentiometric apparatus to avoid systematic errors and to check for reproducibility. All solutions were freshly prepared.

Calculations

The calculations for calibrating the electrode system were performed using the ACBA program,[15] which refines the parameters of an acid–base titration by using a non-linear least-squares method minimizing the function $U = \Sigma(V_{exptl} - V_{calc})^2$, where V is the volume of titrant added. The program SUPERQUAD,[16] which minimizes the error-square sum based on measured electrode potentials, was used to handle all other data. The distribution diagrams were obtained using DISDI.[17]

ESR measurements

Frozen-solution ESR spectra were recorded on a type ER 200 D Bruker instrument driven by the 3220 data system, 150 K achieved by the aid of a standard low-temperature apparatus. Complex solutions (5 mmol dm^{-3}) were prepared by mixing aqueous solutions of $^{63}Cu(NO_3)_2 \cdot 6H_2O$ and the cyclopeptide in 1:1 ratio and adjusting the pH at those values, known from the pH metric measurements, which allow one to handle one species at a time. Furthermore, spectra were recorded for solutions in which the copper(II) to cyclopeptide ratio was 1:2 at pH values near neutrality (≈7.3). The cyclopeptide was first dissolved in acidic (pH 2) aqueous solution, in order to ensure the fully protonated species, and then, after the addition of the copper(II) ion solution, the pH was slowly raised to the desired value by adding KOH. Up to 10% methanol was added to increase resolution which is known to be poor for aqueous solutions. Parallel spin-Hamiltonian parameters were calculated directly from the computer output of the experimental spectra. Diphenylpicrylhydrazyl (dpph) radical ($g = 2.0036$) was used to standardize the klystron frequency, the magnetic field being monitored by a Bruker type ER 035 M gauss meter.

Superoxide dismutase activity measurements

Superoxide dismutase-like activity was determined indirectly using the method of Beauchamp and Fridovich.[18] Superoxide ions were generated by the xanthine–xanthine oxidase system and detected spectrophotometrically by monitoring the formation of formazan as the reduction product of nitro blue tetrazolium at 560 nm. Reactions were carried out with nitro blue tetrazolium (100 μmol dm^{-3}) and xanthine (50 μmol dm^{-3}) in a phosphate buffer (10 mmol dm^{-3}) at pH 7.4. An appropriate amount of xanthine oxidase was added to the reaction mixture (2 cm^3) to cause a change in absorbance (ΔA_{560}) of 0.024 unit min^{-1}, corresponding to a rate of production of O_2^- of 1.2 μmol dm^{-3} min^{-1}. The nitro blue tetrazolium reduction rate was determined for 300 s, both in the presence and absence of the copper(II) complexes. All experiments were carried out at 25 ± 0.2 °C using 1 cm thermostatted cuvettes, in which solutions were magnetically stirred. In separate experiments uric acid production by xanthine oxidase were monitored spectrophotometrically at 298 nm, ruling out any inhibition of xanthine oxidase activity by these systems. Absorption measurements were carried out on an HP-8452A diode-array spectrophotometer.

Voltammetric measurements

Cyclic voltammograms were obtained by an Amel model 473 instrument equipped with a three-electrode system, a 3 mm diameter glassy-carbon disc as working electrode, a saturated calomel electrode (SCE) as reference and a platinum electrode as auxiliary electrode, respectively. Complex solutions (1 mmol dm^{-3}) were prepared in twice-distilled water, as explained above, using 100 mmol dm^{-3} KNO_3 as supporting electrolyte. Cyclic voltammograms at 25 ± 0.1 °C were recorded in the region from +1.0 to −1.0 V *versus* SCE, varying the sweep rate from 10 to 200 mV s^{-1} to characterize the number of electrons involved in the electron-transfer process.

Table 1 Values of log β for proton and copper(II) complexes with L^1 and L^2 at 25 °C and I = 0.1 mol dm^{-3} (KNO_3) with estimated standard deviations in parentheses

Reaction	log β
$L^1 + H^+ \rightleftharpoons [HL^1]^+$	7.28(1)
$L^1 + 2H^+ \rightleftharpoons [H_2L^1]^{2+}$	13.82(2)
$Cu^{2+} + L^1 + H^+ \rightleftharpoons [Cu(HL^1)]^{3+}$	11.09(2)
$Cu^{2+} + L^1 \rightleftharpoons [CuL^1]^{2+}$	6.65(1)
$Cu^{2+} + 2L^1 \rightleftharpoons [CuL^1_2]^{2+}$	11.53(3)
$Cu^{2+} + L^1 \rightleftharpoons [CuL^1H_{-1}]^+ + H^+$	−0.28(1)
$Cu^{2+} + L^1 \rightleftharpoons [CuL^1H_{-2}] + 2H^+$	−8.39(2)
$L^2 + H^+ \rightleftharpoons [HL^2]^+$	7.17(1)
$L^2 + 2H^+ \rightleftharpoons [H_2L^2]^{2+}$	13.76(2)
$Cu^{2+} + L^2 + H^+ \rightleftharpoons [Cu(HL^2)]^{3+}$	10.97(2)
$Cu^{2+} + L^2 \rightleftharpoons [CuL^2]^{2+}$	6.49(1)
$Cu^{2+} + 2L^2 \rightleftharpoons [CuL^2_2]^{2+}$	11.20(3)
$Cu^{2+} + L^2 \rightleftharpoons [CuL^2H_{-1}]^+ + H^+$	−0.40(1)
$Cu^{2+} + L^2 \rightleftharpoons [CuL^2H_{-2}] + 2H^+$	−8.79(2)

Results and Discussion

Thermodynamic results

Proton complexes. Protonation constants involving both imidazole nitrogens are given in Table 1. The values determined for the two cyclopeptides are very similar, and suggest that the different numbers of methylene groups, one for L^1 and two for L^2, between the diketopiperazine ring and the amide group in their side chains does not play a crucial role. Owing to this small difference, hereafter the protonation equilibria of the two systems will be discussed together.

To the best of our knowledge, both protonation constants are the highest among those reported for histidine or histamine-containing linear peptides.[19,20] In particular, the first protonation step is about 0.3 logarithmic units higher whereas the second is about 0.6 units higher with respect to analogous steps reported in the literature. This behaviour leads to an unusually small difference between the two steps. It is well known that for peptides containing two histadines, normally the second protonation step is much lower than the first (about 1.0 log unit). The average difference between the first and second protonation steps for L^1 and L^2 is about 0.66 log units. In fact, the second protonation step is 6.5–6.6 log units against the normal value which is lower than 6.0 log units.

Different factors can play a role in increasing the protonation constants, such as the presence of neighbouring charges, the formation of hydrogen bonds or the occurrence of other weak interactions. Recently, Boschcov *et al.*[21] have considered the influence of charge on the log K of histidines and histamines. Their conclusion is that the absence of an adjacent, positively charged amino group raises the log K of the imidazole nitrogen. However, the log K of glycylhistamine is 'only' 6.78. For this peptide the influence of the positive charge on the terminal protonated amino group can be considered almost negligible, owing to its distance from the imidazole. Therefore, the high protonation constants found for both the present cyclopeptides cannot be merely explained by the absence of close positive groups. Most likely, other factors (such as hydrogen-bond formation or solvation processes) may contribute to these 'anomalous' values. Calorimetric measurements are in progress to gain a better insight.

Copper(II) complexes. For copper(II) complexation we obtained the same set of stability constants with both cyclopeptides (Table 1). The 'best' fit for each system was obtained considering the species $[Cu(HL)]^{3+}$, $[CuL]^{2+}$, $[CuL_2]^{2+}$, $[CuLH_{-1}]^+$ and $[CuLH_{-2}]$, where L = L^1 or L^2. We have also made measurements on solutions containing a metal to peptide ratio of 2:1, but no binuclear species were detected. A species distribution diagram (Fig. 1) shows that the major species in the range pH 4.5–7.0 is $[CuL]^{2+}$. The stability constant for this species is much lower than those reported for copper(II)–L-histidyl-L-histidine[22] or -glycyl-L-histidyl-glycyl-L-histidine[19] complexes and slightly higher than that for copper(II)–cyclo(-L-histidyl-L-histidyl-).[23] In the first two complexes copper(II) is proposed to be co-ordinated to three and four nitrogens, respectively, to only two nitrogens in the latter. Therefore, we can assume that only the two imidazole nitrogens are involved in the co-ordination of the present $[CuL]^{2+}$ species. The slightly higher value for the present complexes compared to that of the analogous complex with cyclo(-L-histidyl-L-histidyl-) can be most likely attributed to the co-ordination of copper(II) to the two carbonyl oxygen atoms of the 'side chain' amide groups. This particular feature leads to the formation of an eleven-or thirteen-membered ring with L^1 and L^2, respectively. The formation of rings of similar dimensions is unusual [it has been previously observed for cyclo(-L-histidyl-L-histidyl-)][23] and in a certain way recalls what happens in proteins, *i.e.* metal ions are co-ordinated to binding sites which are remote in the primary structure.

The $[CuL_2]^{2+}$ species forms in the same pH range in which $[CuL]^{2+}$ exists. It occurs in very low percentages when the metal to L ratio is 1:1, but with increasing relative concentration of L its percentage increases and it becomes the major species at pH around 7, as shown in Fig. 2. In the pH range 5–7, the $[CuLH_{-1}]^+$ and $[CuLH_{-2}]$ species start to form. The log deprotonation constant for this reaction

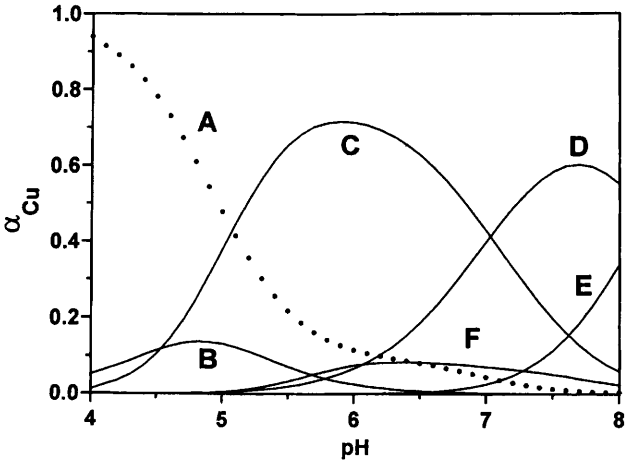

Fig. 1 Species distribution diagram for the copper(II)–L^1 system. $[Cu]^{2+} = [L^1]$ = 4 mmol dm^{-3}. **A** = Cu^{2+}, **B** = $[Cu(HL)]^{3+}$, **C** = $[CuL]^{2+}$, **D** = $[CuLH_{-1}]^+$, **E** = $[CuLH_{-2}]$, **F** = $[CuL_2]^{2+}$

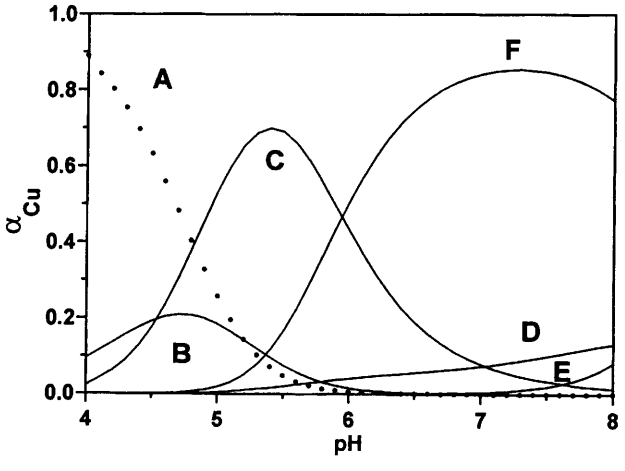

Fig. 2 Species distribution diagram for copper(II)–L^1 system. $[Cu]^{2+}$ = 4 mmol dm^{-3}, $[L^1]$ = 8 mmol dm^{-3}. Complex species as in Fig. 1

($[CuL]^{2+} \rightleftharpoons [CuLH_{-1}]^{+} + H^{+}$) is < 7.0 and therefore is consistent with the deprotonation of an amide nitrogen. Most likely, owing to their proximity, the nitrogen atoms involved in the co-ordination to copper are those of the amide groups of the side chains.

ESR spectroscopic measurements

From the data in Table 2, the ESR spectra of these systems reveal many species depending on the pH of the aqueous solution, as already found by the pH-metric study. The successive deprotonation of the imidazole and amide nitrogen atoms in both cyclopeptides gives the possibility of the formation of different co-ordination sites available to copper(II) ions. We are mainly interested in the adducts with four-nitrogen environments, which can be obtained in 1:1 or 2:1 metal to ligand ratios at pH values near neutrality. The other complex species are not very important for this work. Since $g_{\|} > g_{\perp} > 2.04$, these species have the usual tetragonally elongated octahedra with a $d_{x^2-y^2}$ ground state which is characteristic of the majority of copper(II) complexes. The

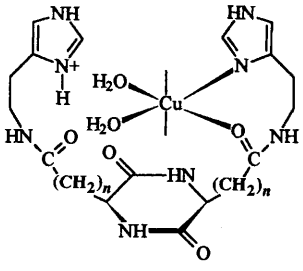

B
$[Cu(HL)]^{3+}$

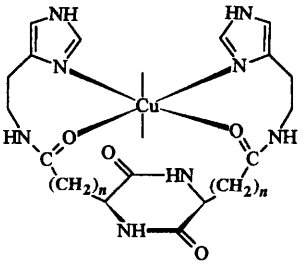

C
$[CuL]^{2+}$

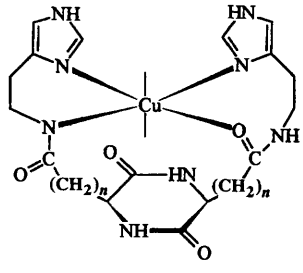

D
$[CuLH_{-1}]^{+}$

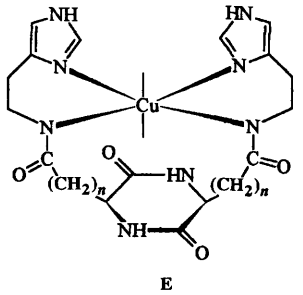

E
$[CuLH_2]$

decrease in $g_{\|}$ and the relative increase in $A_{\|}$ on going to higher pH is the result of the successive co-ordination of imidazole or amide nitrogen atoms. Species **B** probably involves the co-ordination of one imidazole nitrogen and a carbonyl oxygen atom, the remaining equatorial and apical positions being occupied by water molecules. In **C** two nitrogen and two carbonyl oxygen atoms symmetrically co-ordinate the copper(II) in the equatorial plane. The relatively low $A_{\|}$ value for these CuN_2O_2 chromophores suggests distortion of this site towards a tetrahedral situation. Species **D** forms when one of the two amide nitrogen atoms begins to deprotonate and has a $CuN_2N'O$ chromophore. The decrease in $g_{\|}$ as well as the noteworthy increase in $A_{\|}$ represents the contribution to the ligand field caused by the entrance of the peptide nitrogen atom into the co-ordination sphere of the complex. On raising the pH again a fourth species **E** is obtained. At this stage two species should be present, as ascertained by the speciation study at room temperature, but as often occurs low temperatures favour the most stable species.[24] The magnetic parameters are typical of a copper(II) complex co-ordinated by four nitrogen atoms in the equatorial plane, especially the large value of $A_{\|}$ which compares well with values found for similar systems.[25] In this species a $CuN_2N'_2$ chromophore can be considered to be present. In fact, the complexes with both L^1 and L^2 show superhyperfine structure, arising from the interaction of the copper(II) odd electron with four nitrogen donor atoms, as can be seen from their spectra in Figs. 3 and 4. There are differences between the **E** species depending on the ligand: (*i*) the superhyperfine structure is better resolved when L^2 is present [see Fig. 4(*a*)]; (*ii*) the $g_{\|}$ value for the copper(II) complex with L^1 is higher. Both facts could indicate a possible tetrahedral perturbation of the copper(II) site when it is bound to the latter ligand. The shorter length of the methylene chains could probably cause constraints to the stereochemical arrangement of $[CuL'_2H_{-2}]$.

When the copper(II) to ligand ratio is 1:2 the ESR spectra of the two resulting species are quite similar (see Fig. 5) and the spin-Hamiltonian parameters are given in Table 3. By comparison with the copper(II)–imidazole system[24] {for $[Cu(Him)_4]^{2+}$ $g_{\|} = 2.260$, $A_{\|} = 185 \times 10^{-4}$ cm^{-1}, $g_{\perp} = 2.054$, $A_{\perp} = 17 \times 10^{-4}$ cm^{-1}, $A_{\|}^{N} = 16 \times 10^{-4}$ cm^{-1}, $A_{\perp}^{N} = 12 \times 10^{-4}$ cm^{-1}} it is possible to state that these species only involve the co-ordination of imidazole nitrogen atoms which are certainly the more disposable donor atoms. By comparison with the preceding $[CuLH_{-2}]$ complexes having four-nitrogen co-ordination, it is possible to assert that the relatively greater $g_{\|}$ values and lower $A_{\|}$ constants reflect the fact that peptide nitrogens are no longer present and the lower $A_{\|}$ hyperfine constants reflect a slightly tetrahedral perturbation of the co-ordination sphere. Also in this case the frozen-solution ESR spectra revealed superhyperfine structure due to the presence of four nitrogens, more evident for the copper(II) complex with L^2 [see Fig. 4(*b*)].

Table 2 Spin-Hamiltonian parameters for copper(II) complexes with L^1 or L^2 in water-methanol (9:1) at 150 K, on varying the aqueous solution pH

		L^1		L^2	
pH	Complex species	$g_{\|}$	$A_{\|}$*	$g_{\|}$	$A_{\|}$*
5.5–6.0	**B**	2.367(2)	132(3)	2.374(2)	134(3)
5.8–6.2	**C**	2.316(2)	142(3)	2.325(2)	139(3)
6.0–6.5	**D**	2.295(2)	175(2)	2.294(2)	173(2)
6.5–7.8	**E**	2.253(2)	199(2)	2.220(2)	197(2)

Presumed errors on the last digit are given in parentheses. Species **B**, **C**, **D** and **E** correspond to $[Cu(HL)]^{3+}$, $[CuL]^{2+}$, $[CuLH_{-1}]^{+}$ and $[CuLH_{-2}]$, respectively. * Hyperfine coupling constants are in units of 10^4 cm^{-1}.

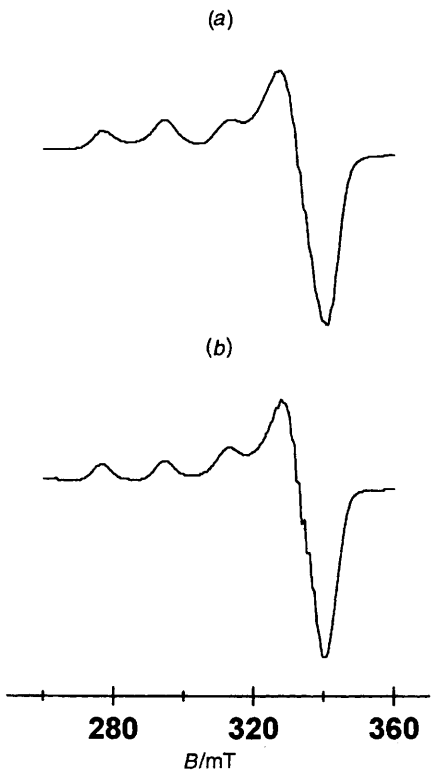

Fig. 3 Frozen-solution ESR spectra of the copper(II) complexes with L^2 (*a*) and L^1 (*b*) in 1:1 metal to ligand ratio at pH 7.7. Microwave frequency = 9.442 GHz, modulation frequency = 100 kHz, modulation amplitude = 0.63 mT, time constant = 0.5 s, microwave power = 20 mW

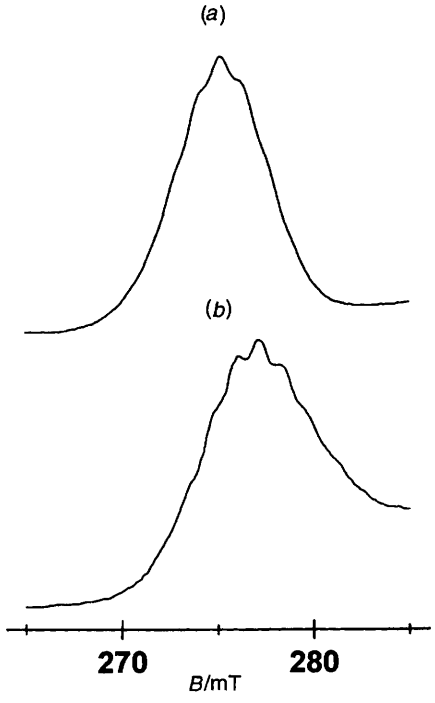

Fig. 4 Frozen-solution ESR spectra of the lowest-field feature for copper(II) complexes with L^2 obtained from aqueous solutions with metal to ligand ratios of 1:1 (*a*) and 1:2 (*b*) at pH 7.3–7.7. Instrument settings in (*a*) and (*b*): microwave frequency = 9.442 and 9.549 GHz, modulation frequency = 100 kHz, modulation amplitude = 0.2 and 0.149 mT, time constant = 0.3 and 0.327 s, microwave power = 20 mW

The visible spectra of these complexes confirmed what has been said on the basis of their ESR spectra. At a 1:1 copper:ligand ratio, λ_{max} shifts towards the red for the L^1 system, consistent with the supposed tetrahedral distortion

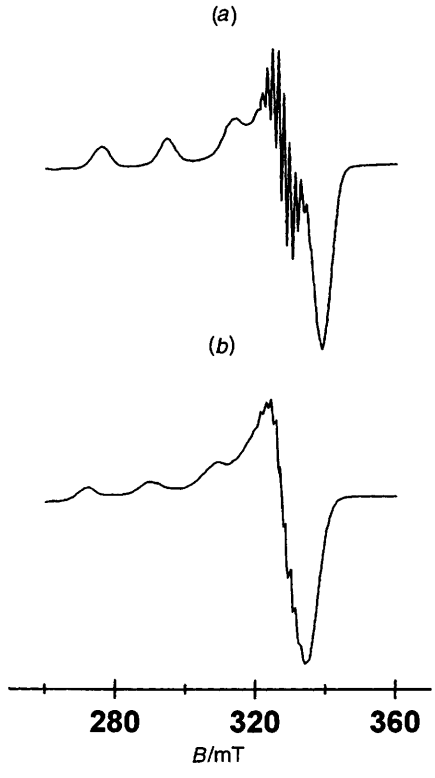

Fig. 5 Frozen-solution ESR spectra of copper(II) complexes with L^2 (*a*) or L^1 (*b*) in 1:2 metal to ligand ratio at pH 7.3. Microwave frequency = 9.549 GHz, modulation frequency = 100 kHz, modulation amplitude = 0.149 mT, time constant = 0.327 s, microwave power = 20 mW

Table 3 Spin-Hamiltonian parameters of copper(II) complexes with L^1 or L^2 (1:1 and 1:2 copper to ligand ratio) in water–methanol (9:1) at 150 K, at pH 7.3–7.7

	L^1		L^2	
Cu:L	1:1	1:2	1:1	1:2
$g_{\|}$	2.253(2)	2.246(2)	2.220(2)	2.247(2)
$10^4 A_{\|}/cm^{-1}$	199(2)	190(2)	197(2)	189(2)
$g_{\perp}$	2.061(4)	2.045(4)	2.043(4)	2.042(4)
$10^4 A_{\perp}/cm^{-1}$	16(4)	15(4)	15(4)	16(4)
$10^4 A_{\|}^N/cm^{-1}$	16(2)	17(2)	17(2)	16(2)
$10^4 A_{\perp}^N/cm^{-1}$	—	—	12(2)	12(2)
λ_{max}/nm	630(2)*	602(2)	588(2)*	612(2)
$\varepsilon_{max}/dm^3\ mol^{-1}\ cm^{-1}$	63(5)*	44(5)	74(5)*	48(5)

Presumed errors on the last digit are given in parentheses. * Since at pH 7.3–7.7 different species, $[CuL]^{2+}$, $[CuLH_{-1}]^+$ and $[CuLH_{-2}]$, are present, the wavelength and molar absorption coefficients are average values for these.

undergone by the copper site, even if it must be considered that at least $[CuL]^{2+}$, $[CuLH_{-1}]^+$ and $[CuLH_{-2}]$ contribute to the overall absorption. In the case of $[CuL_2]^{2+}$ species with L^1 or L^2, there were only subtle differences which could be due to small constraints experienced by the two copper(II) co-ordination sites.

Voltammetric data

The reduction processes of these complexes were electrochemically irreversible because they are complicated by structural rearrangements or a probable dissociation reaction as demonstrated by the fact that reduced copper(I) species was never reoxidized at the expected anodic potential values for one-electron transfers. The cathodic potential values varied, in particular becoming more negative as the potential sweep rate

increased from 10 to 200 mV s^{-1}, as expected for an irreversible process. However, the electrode processes are diffusion controlled since the temperature coefficient is less than 2% per degree; in particular, it was 1.1 ± 1.3% in the range 25–55 °C, so the electron transfer could perhaps be considered as quasi-reversible. From the variation of the cathodic current with the potential sweep rate it was possible to conclude that all these processes involve the transfer of one electron. An anodic peak with comparable current was detected at more positive potentials, which did not lie at the potential of free copper and, thus, is ascribed to the oxidation of a copper(I) complex with a different level of co-ordination. In other words, a structural rearrangement of the reduced copper(I) complex occurs, owing to its geometrical requirements. In particular, this reduced copper(I) complex could assume a typical tetrahedral stereochemistry or some of the donor atoms of the ligand may temporarily leave the co-ordination sphere, giving a linear complex. Moreover, successive scans did not reveal a different behaviour, thus we can exclude the possibility of a disproportionation reaction of the copper(I) species. No peaks due to free copper(II) reduction were ever detected in successive scans. Therefore, it seems reasonable that during the reduction process a stereochemical rearrangement occurs, but when this new copper(I) species is reoxidized, the original copper(II) complex is fully restored. This would account for the catalytic activity shown by these species in the presence of an almost irreversible electron transfer. Fig. 6 shows typical voltammetric patterns obtained with the copper(II) mono and bis complexes of L^1 at pH ≈ 7.3–7.7. Table 4 gives the peak potentials and the relative peak currents for each of the complex species at a sweep rate of 50 mV s^{-1}. Within a similar redox pattern, the bis complexes showed reduction potentials which were lower than those of the mono species, as expected for more easily reducible species. At a Cu:L ratio of 1:1 the speciation study gives a mixture of complex species at pH ≈ 7.3–7.7, in particular $[CuL]^{2+}$, $[CuLH_{-1}]^{+}$ and $[CuLH_{-2}]$, so the reduction potential values are averaged over these species.

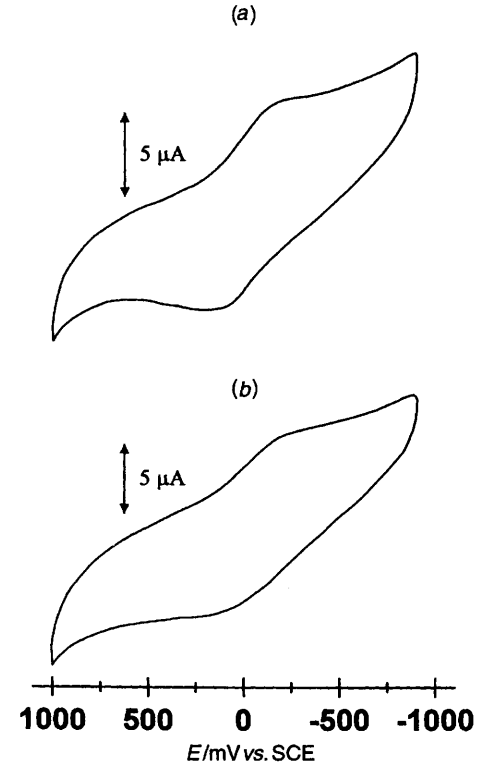

Fig. 6 Cyclic voltammograms associated with copper reduction from 1 mmol dm^{-3} complex solutions for the Cu–L^1 system recorded at a glassy carbon electrode with 100 mmol dm^{-3} KNO_3 as supporting electrolyte, at pH ≈ 7.3–7.7. Potential sweep rate 50 mV s^{-1}. Copper: ligand ratio = 1:2 (*a*) and 1:1 (*b*)

Some of us have recently shown[25] that this redox behaviour is typical of copper(II) complexes with biofunctional ligands. In particular, when the complex co-ordination sphere contained deprotonated amide nitrogens, the reoxidation process often did not give the original complex species and sometimes resulted in degradation of the ligand itself.

Superoxide dismutase-like activity

In previous works[19] we have shown that only a knowledge of the speciation of the system permits one to understand which are the most active species. Hence, we do need to know which species are to be considered and their relative proportions under the experimental conditions of the indirect assay. Furthermore, we have also to consider copper(II) species which may form with the buffer (phosphate in this case) and with xanthine.

The I_{50} value (the concentration causing 50% inhibition of nitro blue tetrazolium reduction; *i.e.* ΔA_{560} = 0.012 unit min^{-1}) for Cu–L^1 and Cu–L^2 systems has been found to be 2.5 × 10^{-7}, when a 1:1000 metal to ligand ratio (R) is considered. Table 5 gives the percentage of the copper(II) species existing under the experimental conditions of the indirect assay for SOD activity (10 mmol dm^{-3} phosphate buffer, pH 7.4 and 50 μmol dm^{-3} xanthine) together with the scavenger activity against O_2^- radicals at different metal to ligand ratios. Considering that for these systems the I_{50} value is obtained at R = 1:1000 (in other words we have 100% scavenger activity), it is evident that the SOD-like activity increases with cyclopeptide concentration.

Table 5 shows that the only species which grows with cyclopeptide concentration is $[CuL_2]^{2+}$. The best result is obtained when the percentage of this species is maximum, therefore it is reasonable to assume that it does show the greatest catalytic activity. However, it is not simple to explain this. One factor which can discriminate among the catalytic features of these copper(II) species could be the flexibility of the copper(II) arrangement, which facilitates the interaction of the O_2^- radical, followed by the rapid electron transfer reaction which results in reduction to copper(I) species, and certainly the bis species has the most flexible co-ordination sites. As some of us have recently shown[26] for the interaction of H_2O_2 with copper(II) complexes containing one or two amide bonds, copper in its monovalent state 'doesn't like' to be bound to amide nitrogens, which impose planar co-ordination. The electrochemical data, too, confirmed this interpretation, showing that the easily reducible species were the bis complexes. However, such electrochemical data must be interpreted with great care, because the catalytic activity involved reduced species through the formation of unstable adducts, followed by rapid electron transfers. Interestingly, the electrochemical behaviour of these complexes suggested that the reduction process occurred through a stereochemical rearrangement or a

Table 4 Voltammetric data at 25 °C for ≈1 mmol dm^{-3} copper(II) complexes with L^1 or L^2 in aqueous solution (pH 7.3–7.7) at 1:1 and 1:2 copper(II) to ligand ratio, with 100 mmol dm^{-3} KNO_3 as supporting electrolyte, at 50 mV s^{-1}

	L^1		L^2	
Cu:L	1:1[a]	1:2	1:1[a]	1:2
E_{p_c}[b]/V *vs.* SCE	−0.29	−0.25	−0.32	−0.12
i_{p_c}[b]/μA	5.0	5.2	5.9	5.7
E_{p_a}[b]/V *vs.* SCE	+0.26	+0.19	+0.23	+0.32
i_{p_a}[b]/μA	—	4.9	6.3	5.9

[a] Since at pH 7.3–7.7 different complex species, $[CuL]^{2+}$, $[CuLH_{-1}]^{+}$, $[CuLH_{-2}]$, are present the potentials and currents are average values for the reduction of these species. [b] Owing to not well defined peaks, the presumed errors are ±0.015 V on peak potentials and ± 10% on peak currents.

Table 5 Percentages of copper(II) complexes existing under the experimental conditions of the xanthine (xa)–xanthine oxidase indirect assay for superoxide dismutase activity (1 mmol dm^{-3} phosphate buffer, pH 7.4, $[Cu]^{2+}$ = 0.25 μmol dm^{-3}) and SOD-like activity

		Species [a] (%)					
L	M:L	[Cu(xa)]	[CuL]	CuL_2]	$[CuLH_{-1}]$	$[CuLH_{-2}]$	Activity[b]
L^1	1:10	10	20	1	59	10	20
	1:100	—	18	18	53	10	40
	1:1000	—	7	69	20	4	100
L^2	1:10	10	18	2	58	6	20
	1:100	—	19	14	60	6	40
	1:1000	—	8	63	26	3	100

[a] Charges omitted for simplicity. [b] 100 represents the experimental conditions at which I_{50} is obtained.

partial dissociation of the complexes, but at the end of the entire voltammetric cycle the original complex is fully restored.

Another factor could be, as previously hypothesized,[25] the possibility of the formation of other species having different co-ordination levels or degraded ligands which continue to show catalytic activity, after the interaction with O_2^- has occurred. Also in this case, the bis complex would be favoured because other species are more easily derived from it.

The I_{50} value measured for the bis complex is among the highest available in the literature for copper(II) complexes showing antioxidant activity and is 'only' six times lower that that determined for SOD.[27]

Acknowledgements

We thank the EEC HCM project, contract number CHRXCT920014, for supporting this work. We acknowledge the discussion of the results of this work with our partners in brief but fruitful EEC meetings. Consiglio Nazionale delle Ricerche (CNR, Rome) and Ministero della Università e della Ricerca Scientifica e Tecnologica (MURST) are also acknowledged for providing partial support.

References

1 J. M. McCord and I. Fridovich, *J. Biol. Chem.*, 1968, **243**, 5753.
2 J. M. McCord and I. Fridovich, *J. Biol. Chem.*, 1969, **244**, 6049.
3 P. F. Knowles, J. F. Gibson, F. M. Pick and R. C. Bray, *Biochem. J.*, 1969, **111**, 53.
4 J. M. McCord. *Science*, 1974, **185**, 529.
5 L. W. Oberley and G. R. Buettner, *Cancer Res.*, 1979, **39**, 1141.
6 T. C. Pederson and S. D. Aust, *Biochem. Biophys. Res. Commun.*, 1973, **52**, 1071.
7 B. G. Que, K. M. Doweney and A. G. So, *Biochemistry*, 1980, **19**, 5987.
8 I. Fridovich, *Science*, 1978, **201**, 875.
9 I. Fridovich, *Adv. Inorg. Biochem.*, 1979, **1**, 67.
10 J. A. Tainer, E. D. Getzoff, J. S. Richardson and D. C. Richardson, *Nature (London)*, 1983, **306**, 284.
11 S. Mangani, P. L. Orioli and P. Carloni, *Inorg. Chim. Acta*, 1994, **216**, 121.
12 J. R. Dorfman, R. D. Bereman and M. Whanyho, in *Coordination Chemistry: Biochemical and Inorganic Perspectives*, eds. K. K. Karlin and J. Zubieta, Adenine Press, New York, 1983, p. 75.
13 J. C. Touchstone and M. F. Dobbins, *Practice of Thin Layer Chromatography*, 2nd edn., Wiley-Interscience, New York, 1983.
14 A. Flaschka, *EDTA Titrations*, Pergamon, London, 1959.
15 G. Arena, C. Rigano, E. Rizzarelli and S. Sammartano, *Talanta*, 1979, **26**, 1.
16 P. Gans, A. Vacca and A. Sabatini, *J. Chem. Soc., Dalton Trans.*, 1985, 1195.
17 R. Maggiore, S. Musumeci and S. Sammartano, *Talanta*, 1976, **23**, 43.
18 C. Beauchamp and I. Fridovich, *Anal. Biochem.*, 1971, **44**, 276.
19 R. P. Bonomo, F. Bonsignore, E. Conte, G. Impellizzeri, G. Pappalardo, R. Purrello and E. Rizzarelli, *J. Chem. Soc., Dalton Trans.*, 1993, 1295 and refs. therein.
20 T. Gajda, B. Henry and J.-J. Delpuech, *J. Chem. Soc., Dalton Trans.*, 1993, 1301.
21 P. Boschcov, W. Seidel, J. Muradian, M. Tominaga, A. M. C. Paiva and L. Juliano, *Bioorg. Chem.*, 1983, **12**, 34.
22 C. E. Livera, L. D. Pettit, M. Bataille, B. Perly, H. Kozlowski and B. Radomska, *J. Chem. Soc., Dalton Trans.*, 1987, 661.
23 G. Arena, R. P. Bonomo, G. Impellizzeri, R. M. Izatt, J. D. Lamb and E. Rizzarelli, *Inorg. Chem.*, 1987, **26**, 795.
24 R. P. Bonomo, F. Riggi and A. J. Di Bilio, *Inorg. Chem.*, 1988, **27**, 2510.
25 R. P. Bonomo, E. Conte, R. Marchelli, A. M. Santoro and G. Tabbì, *J. Inorg. Biochem.*, 1994, **53**, 127.
26 R. P. Bonomo, R. Marchelli, and G. Tabbì, *J. Inorg. Biochem.*, 1995, **60**, 805.
27 U. Deuschle and U. Weser, *Prog. Clin. Biochem. Med.*, 1985, **2**, 97.

Received 15*th January* 1996; *Paper* 6/00302H